Vol 14 No 10, October 2005
1009-1963/2005/14(10)/2122-05

Chinese Physics

© 2005 Chin. Phys. Soc.
and IOP Publishing Ltd

Effect of composition on the crystallographic texture and magnetic properties of the $Sm(Co,Fe,Cu,Zr)_z$ ribbons prepared by simple processing*

Rong Chuan-Bing(荣传兵)[a)†], He Shu-Li(贺淑莉)[a)b)], Chen Ren-Jie(陈仁杰)[a)], Zhang Hong-Wei(张宏伟)[a)], and Shen Bao-Gen(沈保根)[a)]

[a)] *State Key Laboratory of Magnetism, Institute of Physics and Centre for Condensed Matter Physics, Chinese Academy of Sciences, Beijing* 100080, *China*

[b)] *Department of Physics, Capital Normal University, Beijing* 100037, *China*

(Received 3 June 2005; revised manuscript received 28 June 2005)

$Sm(Co_{bal}Fe_yCu_xZr_w)_z$ ribbons have been prepared by melt spinning at a low wheel velocity followed by short-time aging and slow cooling the as-spun ribbons from 850 to 400°C. It is found that the composition can significantly influence the degree of crystallographic texture of the ribbons. The 1:7 phase of the as-spun ribbons is segregated into 1:5 and 2:17 phases by the simple processing procedure. However, the crystallographic texture is still preserved in the ribbons after precipitation hardening. $(BH)_{max}$ about 86kJ/m^3 can be obtained in the Sm(Co, Fe, Cu, Zr)$_z$ ribbons by the adjustment of composition.

Keywords: permanent magnets, melt spinning, magnetic properties, precipitation hardening
PACC: 7550V, 8140

1. Introduction

The search for novel soft and hard magnetic materials for high-temperature advanced power applications is worldwide an active area of research. In the development of high temperature magnets the activities concentrate on the improvement of existing hard magnetic materials, such as the precipitation hardened Sm(Co, Fe, Cu, Zr)$_z$ magnets, and on the search for new compounds with sufficiently high values of magnetization and coercivity at elevated temperatures. Sm(Co, Fe, Cu, Zr)$_z$ permanent magnets are the best choice for operating temperatures above 300°C due to their high magnetocrystalline anisotropy, the strong coercive field and the high Curie temperature.[1−3] The high coercivity results from the coexistence of a cellular microstructure with rhombohedral 2:17 cells surrounded by hexagonal 1:5 cell boundaries. It is generally accepted that the coercivity mechanism of Sm(Co, Fe, Cu, Zr)$_z$ magnets at room temperature is related to pinning of domain walls at the 1:5 phase.[4−6] The complex microstructure of the precipitation-hardened magnets is usually obtained after a lengthy heat treatment. Therefore, some efforts have been undertaken to simplify the processing procedure.[7−9] Unfortunately, the Sm(Co, Fe, Cu, Zr)$_z$ magnets obtained through the simple process is always isotropic. Recently, it has been found that anisotropic magnets (such as RE–Fe–B and Sm–Co systems) can be obtained by a melt-spinning technique at low wheel velocities.[10,11] However, anisotropic precipitation-hardened $SmCo_5/Sm_2Co_{17}$ ribbons have rarely been obtained up to now.[12] Numerous investigations show that the metastable 1:7 phase can by segregated into a mixture of 2:17 and 1:5 phases by precipitation hardening.[13,14] Since the grain-boundary and cellular phases are coherent, the anisotropic Sm(Co, Fe, Cu, Zr)$_z$ magnets may be obtained easily if the anisotropic 1:7-type ribbons can be prepared by melt-spinning. In this paper, the effect of the composition on the crystallographic texture and magnetic

*Project supported by the National Natural Science Foundation of China (Grant No 10274102).
†E-mail:rongcb@g203.iphy.ac.cn

properties of the $Sm(Co_{bal}Fe_{0.1}Cu_{0.1}Zr_w)_7$ ribbons is studied systematically. The coercivity mechanism and the exchange interaction in these precipitation-hardened magnets will be discussed in detail in another paper.

2. Experiments

Ingots with nominal composition $Sm(Co_{bal}\ Fe_y\ Cu_x\ Zr_w)_z$ with $x = 0.00 - 0.25$, $y = 0.00 - 0.30$, $w = 0.00 - 0.10$ and $z = 6.5 - 7.5$ were prepared by arc-melting technique. The ribbons were obtained using the single-roller melt-spinning technique with the surface speeds of the Cu wheel about 5 m/s. Subsequently, without the traditional solid solution treatment, they were isothermally aged at 850°C for 3h followed by slow cooling at 1°C/min to 400°C and then quenched to room temperature. Crystalline structure was determined by x-ray diffraction (XRD) with Cu $K\alpha$ radiation. The magnetic properties were measured using a superconducting quantum interference device (SQUID) magnetometer with a maximum applied field of 5T. The field was applied along longitudinal direction of ribbons so the demagnetization factor could be neglected.

3. Results and discussion

3.1. Effect of Cu content

Figure 1 displays typical XRD patterns of the melt-spun and precipitation-hardened $Sm(Co_{bal}\ Fe_{0.1}\ Cu_x\ Zr_{0.03})_7$ ribbons with different Cu contents x. As can be seen from Fig.1(a), the as-spun ribbons consist mainly of a single $TbCu_7$-type phase. This means that the solid solution treatment, which is required for the bulk precipitation-hardened magnets, is not necessary for the melt-spun materials.[8,13,15] The significantly enhanced intensity of the (200) and (110) peaks for the Cu-free ribbon suggests that they are crystallographically anisotropic with easy magnetization direction parallel to the longitudinal direction of the ribbons. However, a small quantity of Cu substitution leads to a significant increase in the intensity of (111) reflection, which is close to that expected for isotropic materials, indicating that no crystallographic texture is present in the ribbons with $x = 0.05$. Further addition of Cu leads to stronger intensity of (111) peak, indicating that the degree of crystallographic texture increases with increasing Cu content.

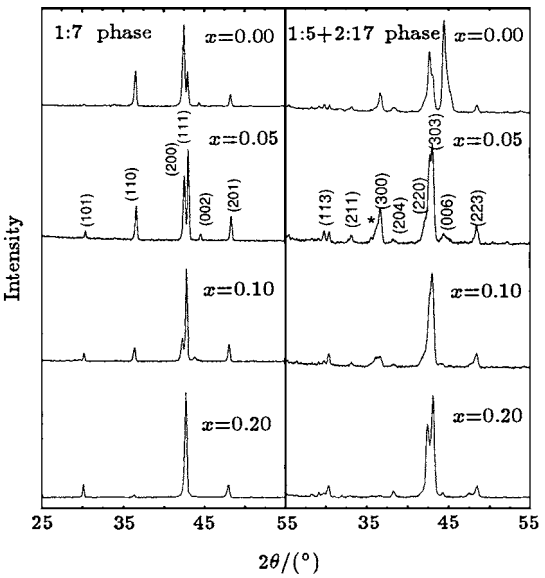


Fig.1. Typical XRD patterns of the melt-spun and precipitation-hardened $Sm(Co_{bal}Fe_{0.1}Cu_xZr_{0.03})_7$ ribbons with different Cu contents.

As shown in Fig.1(b), the 1:7 phase of the melt-spun ribbons is segregated into 1:5 and 2:17 phases after precipitation-hardening. The broadened peaks of the precipitation-hardened samples indicate that phase transformation leads to the formation of a fine microstructure. According to the transmission electron microscopy (TEM) investigations of ours[16–18] and others,[8] it can be concluded that a cellular microstructure is achieved in the ribbons by precipitation-hardening. More interestingly, the XRD patterns of the annealed ribbons are very similar to those of the melt-spun ribbons. This means that the crystallographic texture is still preserved in ribbons after precipitation hardening.

Copper always plays an important role in developing the magnetic properties of the precipitation-hardened magnets.[19] Figure 2 shows the magnetic properties of the precipitation-hardened $Sm(Co_{bal}\ Fe_{0.1}\ Cu_x\ Zr_{0.03})_7$ ribbons as a function of x. As can be seen, the remanence ratio m_r ($= J_r/J_s$ where J_r and J_s are remanence and saturation magnetization, respectively) increases fast with increasing x. The high m_r about 0.8 is obtained in the ribbons with $x = 0.10 - 0.25$. Unfortunately, J_s of the ribbons falls off quickly with increasing x. The coercivity H_c increases slowly with increasing x from 0 to 0.05. When x is increased beyond 0.05, H_c starts increasing significantly and reaches its maximum value about 3 T in the ribbons with $z = 7.5$. It is noted that H_c of the magnets with $z = 7.5$ and 7.0 reaches a maximum when x is 0.15 and 0.20, respectively. However, for the magnets with $z = 6.5$, H_c increases monotonously

with x up to 0.25. Previous studies showed that the magnet with low ratio z has a smaller cell size and the proportion of the cell boundaries is larger.[20] Thus, more Cu is needed to obtain a large domain wall energy gradient across the cell boundaries. This is the reason why the coercivity has not yet reached its maximum even when x is up to 0.25 for the magnets with $z = 6.5$. By adjusting the Cu content, the maximum energy product $(BH)_{max}$ about 80 kJ/m^3 is obtained in the sample with $x = 0.10$ and $z = 7.0$.

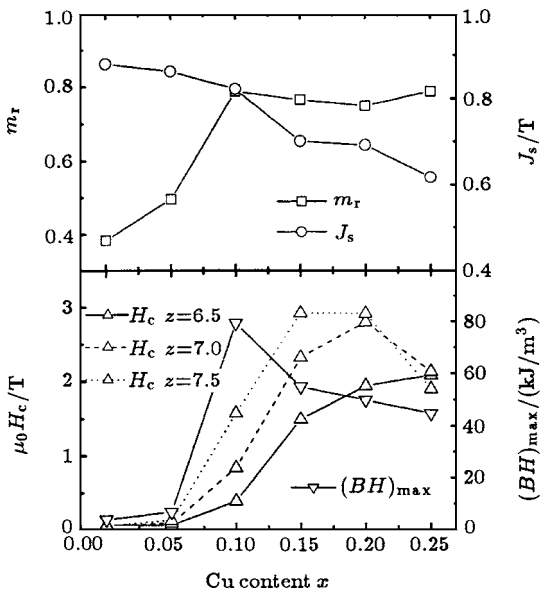


Fig.2. Magnetic properties of the precipitation-hardened $Sm(Co_{bal}Fe_{0.1}Cu_xZr_{0.03})_7$ ribbons as a function of Cu content.

3.2. Effect of Fe content

Figure 3 displays typical XRD patterns of the melt-spun $Sm(Co_{bal}Fe_yCu_{0.1}Zr_{0.03})_7$ ribbons with different Fe contents y. The as-spun ribbons consist mainly of a single $TbCu_7$-type phase. The intensity of the diffraction peaks of the Fe-free ribbon is close to that expected for isotropic materials, indicating that no crystallographic texture is present in the ribbon. The addition of Fe leads to significantly enhanced intensity of (111) peak in the ribbons with $y \leq 0.2$, which indicates the increase of texture degree with increasing y. However, further addition of Fe leads to the disappearance of crystallographic texture in the ribbons.

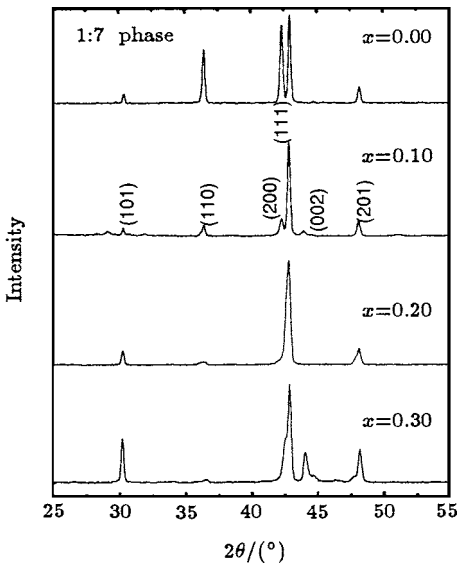


Fig.3. Typical XRD patterns of the melt-spun $Sm(Co_{bal}Fe_yCu_{0.1}Zr_{0.03})_7$ ribbons with different Fe contents.

Previous results suggests that Fe has a significant effect on the magnetic properties since Fe can improve J_s of the Sm(Co, Fe, Cu, Zr)$_z$ magnets. Figure 4 shows the magnetic properties of the precipitation-hardened $Sm(Co_{bal}Fe_yCu_{0.1}Zr_{0.03})_7$ ribbons as a function of y. It shows clearly that addition of Fe can effectively improves J_s. High m_r about 0.8 can be obtained in the ribbons with $y \leq 0.20$. However, m_r decreases fast with further addition of Fe due to the disappearance of crystallographic texture as proved by the XRD patterns. A maximum of coercivity exists with the Fe content $y = 0.15$. The TEM studies for Sm(Co, Fe, Cu, Zr)$_z$ magnets with different y in Ref.[19] show that the magnet with low Fe content has a smaller but non-uniform cell size. With increasing Fe content, the cell size increases but becomes uniform because of Fe substitution in the 2:17 phase. This leads to a larger Cu content in the 1:5 cell boundaries and thus a higher coercivity at a fixed Cu content. With further increase of y, the cell size increases continuously and becomes nonuniform. The cellular structure starts deteriorated, and this leads to the decrease of coercivity. Due to the enhancement of m_r and J_s, $(BH)_{max}$ about 80 kJ/m^3 is obtained in the sample with $y = 0.10 - 0.20$.

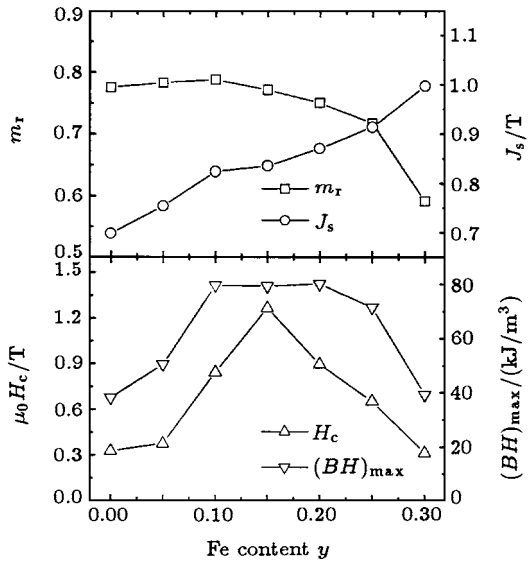


Fig.4. Magnetic properties of the precipitation-hardened $Sm(Co_{bal}Fe_yCu_{0.1}Zr_{0.03})_7$ ribbons as a function of Fe content.

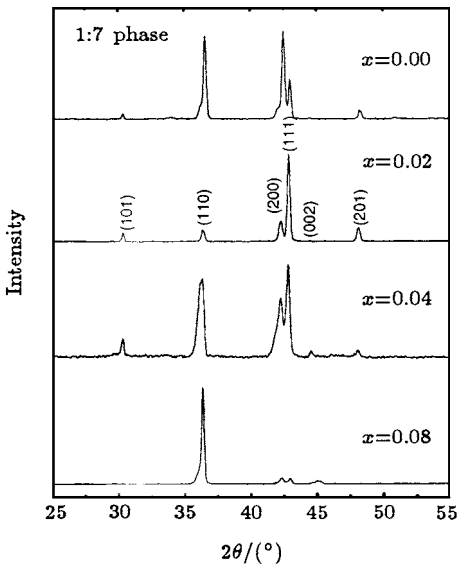


Fig.5. Typical XRD patterns of the melt-spun $Sm(Co_{bal}Fe_{0.1}Cu_{0.1}Zr_w)_7$ ribbons with different Zr contents.

3.3. Effect of Zr content

Figure 5 displays typical XRD patterns of the melt-spun $Sm(Co_{bal}Fe_{0.1}Cu_{0.1}Zr_w)_7$ ribbons with different Zr contents w. All as-spun ribbons consist of a single $TbCu_7$-type phase. The significantly enhanced intensity of the (200) and (110) peaks for the Zr-free ribbon suggests that they are crystallographic anisotropic with easy magnetization direction parallel to the longitudinal direction of the ribbons. However, no obviously preferential orientation of the crystallites is observed from the diffraction peaks of the sample with $w = 0.01$. It is interesting to note that the enhanced intensity of the (110) peak for the sample with $w = 0.04$ suggests that partially preferential orientation is obtained. Further Zr substitution leads to a more pronounced increase in the intensity of (110) peak and the perfect crystallographic texture is obtained in the ribbon with $w = 0.08$. Due to the appearance of 2:7 phase, the crystallographic texture disappears in the ribbon with $w \geq 0.09$.

Figure 6 shows the magnetic properties of the precipitation-hardened $Sm(Co_{bal}Fe_{0.1}Cu_{0.1}Zr_w)_7$ ribbons as a function of w. It is found that m_r of the Zr-free ribbon is as high as 0.84. However, it dramatically decreases to about 0.7 for the sample with $w = 0.01$ and then increases with the increase of w. m_r about 0.9 can be obtained in the ribbons with $w = 0.08$. Further Zr substitution leads to the sharp drop of m_r again. The m_r vs w plot can be attributed to the variation of the texture degree in the ribbons as shown in Fig.5. The coercivity increases significantly with increasing w and reaches the maximum of 1.5 T at $w = 0.06$ due to the increases of the amount of Zr-rich lamellar phase.[20] Unfortunately, Zr addition leads to the fast drop of J_s since J_s of the Zr-rich phase is far lower than that of 1:5 or 2:17 phases.[13] $(BH)_{max}$ at first increases due to the improvement of rectangularity of the demagnetization curves. It reaches a maximum value of about 80kJ/m^3 at $w = 0.03$, and then falls off due to the fast drop of J_s.

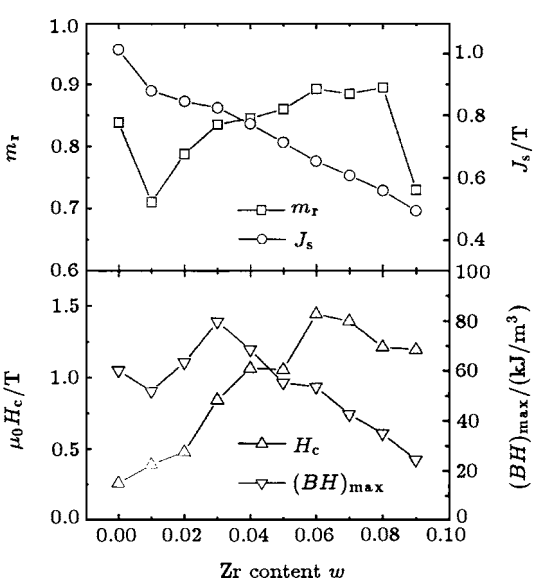


Fig.6. Magnetic properties of the precipitation-hardened $Sm(Co_{bal}Fe_{0.1}Cu_{0.1}Zr_w)_7$ ribbons as a function of Zr content.

3.4. Effect of the ratio z

The XRD patterns of $Sm(Co_{bal}Fe_{0.1}Cu_{0.1}Zr_{0.03})_z$ ribbons, not presented in this paper, show that the Sm content has little influence on the crystallographic texture of the ribbons. Figure 7 shows the magnetic properties of the precipitation-hardened $Sm(Co_{bal}Fe_{0.1}Cu_{0.1}Zr_{0.03})_z$ ribbons as a function of the ratio z. m_r is about 0.8 and rarely influenced by the ratio z. This agrees with the results of XRD patterns. According to the phase diagram,[21] the proportion of the 1:5 cell boundaries is larger for small ratio z. Thus, samples with higher ratio z are found to have higher saturation magnetization because J_s of 2:17 phase is higher than that of 1:5 phases. The TEM studies of Ref.[22] showed that the cell size of the precipitation-hardened magnets increases with the increase of the ratio z. For a fixed Cu content, a larger cell size results in a larger amount of Cu in the 1:5 cell boundaries. This leads to a larger gradient in domain wall energy across the cell boundaries, resulting in a stronger domain wall pinning, and gives rise to a higher coercivity. Due to simultaneous increase of J_s and H_c, $(BH)_{max}$ increases monotonically with increasing ratio z, and a value about 86kJ/m^3 can be obtained in the ribbon with $z = 7.5$.

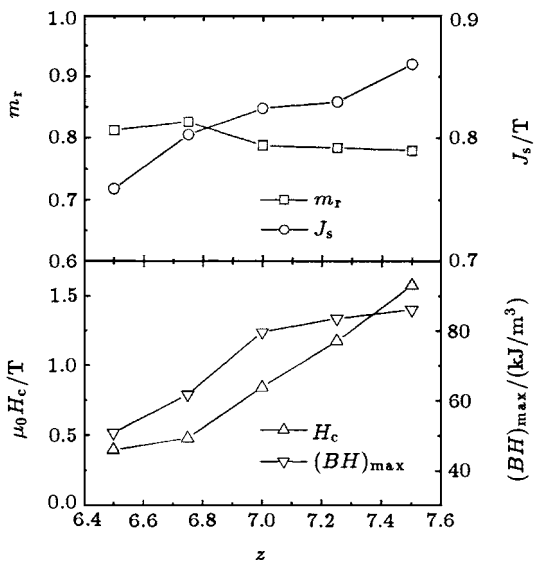


Fig.7. Magnetic properties of the precipitation-hardened $Sm(Co_{bal}Fe_{0.1}Cu_{0.1}Zr_{0.03})_z$ ribbons as a function of the ratio z.

4. Conclusion

The $Sm(Co_{bal}Fe_yCu_xZr_w)_z$ ribbons have been prepared by melt spinning at a low wheel velocity. The as-spun ribbons consist of a single $TbCu_7$-type phase. The composition can significantly influence the crystallographic texture of the ribbons. The 1:7 phase of the melt-spinning ribbons is segregated into 1:5 and 2:17 phases by short time aging and slow cooling the as-spun ribbons from 850 to 400°C. However, the crystallographic texture is still preserved in ribbons after precipitation hardening. $(BH)_{max}$ about 86kJ/m^3 can be obtained in the Sm(Co, Fe, Cu, Zr)$_z$ ribbons obtained by this simple processing procedure.

References

[1] Ray A E and Liu S 1992 *J. Mater. Eng. Perform.* **1** 183

[2] Chen C H, Walmer M S, Walmer M H, Liu S, Kuhl E and Simon G 1998 *J. Appl. Phys.* **83** 6706

[3] Rong C B, Zhang H W, Zhang J, Du X B, Zhang S Y and Shen B G 2004 *J. Appl. Phys.* **95** 1351

[4] Kronmuller H, Durst K -D, Ervens W and Fernengel W 1984 *IEEE. Trans. Magn.* **20** 1569

[5] Rong C B, Zhang H W, Zhang J, Zhang S Y and Shen B G 2003 *Acta Phys. Sin.* **52** 708 (in Chinese)

[6] Chen R J, Rong C B, Zhang H W, He S L, Zhang S Y and Shen B G 2004 *Acta Phys. Sin.* **53** 4341 (in Chinese)

[7] Tang W, Zhang Y and Hadjipanayis G C 2000 *Appl. Phys. Lett.* **77** 421

[8] Yan A, Bollero A, Muller K H and Gutfleisch O 2002 *Appl. Phys. Lett.* **80** 1243

[9] Rong C B, Zhang J, Du X B, Zhang H W, Zhang S Y and Shen B G 2004 *Chin. Phys.* **13** 1144

[10] Dadon D, Gefen Y and Dariel M P 1987 *IEEE Trans. Magn.* **23** 3605

[11] Yan A, Zhang W Y, Zhang H W and Shen B G 2000 *J. Appl. Phys.* **88** 2787

[12] Rong C B, Zhang H W, He S L, Chen R J and Shen B G 2005 *Appl. Phys. Lett.* **86** 122506

[13] Fukui Y, Nishio T and Iwama Y 1987 *IEEE Trans. Magn.* **23** 2705

[14] Rong C B, Chen R J, Zhang H W, Zhang J, Zhang S Y and Shen B G 2004 *J. Phys. D: Appl. Phys.* **37** 3285

[15] Gong W 2000 *J. Appl. Phys.* **87** 6713

[16] Zhang J, Liu H, Rong C B, Zhang H W, Zhang S Y, Shen B G, Bai Y Q and Li B H 2003 *Appl. Phys. Lett.* **83** 1172

[17] Rong C B, Zhang J, Zhang H W, Du X B, Zhang S Y and Shen B G 2004 *J. Magn. Magn. Mater.* **279** 143

[18] Rong C B, Zhang H W, Zhang J, Du X B, Zhang S Y and Shen B G 2005 *J. Appl. Phys.* **97** 33907

[19] Hadjipanayis G C, Tang W, Zhang Y, Chui S T, Liu J F, Chen C and Kronmuller H 2000 *IEEE. Trans. Magn.* **36** 3382

[20] Liu J F, Ding Y, Zhang Y, Dimitar D, Zhang F and Hadjipanayis G C, 1999 *J. Appl. Phys.* **85** 5660

[21] Cataldo L, Lefevre A, Ducret F, Cohen-Adad M-Th, Allibert C and Valignat N 1996 *J. Alloys Compound.* **241** 216

[22] Liu J F, Zhang Y, Dimitrov D and Hadjipanayis G C 1999 *J. Appl. Phys.* **85** 2800